

# **CFD-Analysis Study of Drug Deposition In Tracheobronchial Airways of Asthmatic Persons From Different Age Groups**

A PROJECT REPORT

submitted by

**PRAFUL P**

**TKM21MECI11**

to

the APJ Abdul Kalam Technological University in partial fulfillment of the requirements for the award of the Degree

of

*Master of Technology*

*in*

*Mechanical Engineering with*

*specialisation in*

*Computer Integrated Manufacturing*



**Department of Mechanical Engineering**

TKM College of Engineering  
Kollam

JULY 2023

## DECLARATION

I undersigned hereby declare that the project report entitled "**CFD-ANALYSIS STUDY OF DRUG DEPOSITION IN TRACHEOBRONCHIAL AIRWAYS OF ASTHMATIC PERSONS FROM DIFFERENT AGE GROUPS**", submitted for partial fulfillment of the requirements for the award of degree of Master of Technology in Mechanical Engineering with specialisation in Computer Integrated Manufacturing, of the APJ Abdul Kalam Technological University, Kerala is a bonafide work done by me under the supervision of *Dr.K.E.Reby Roy*, Project Supervisor, Professor, Department of Mechanical Engineering. This submission represents my ideas in my own words and where ideas or words of others have been included. I have adequately and accurately cited and referenced the original sources. I also declare that I have adhered to ethics of academic honesty and integrity and have not misrepresented or fabricated any data or idea or fact or source in my submission. I understand that any violation of the above will be a cause for disciplinary action by the institute and/or the University and can also evoke penal action from the sources which have thus not been properly cited or from whom proper permission has not been obtained. This report has not been previously formed the basis for the award of any degree, diploma or similar title of any other University.

Kollam

July, 2023

PRAFUL P

**DEPARTMENT OF MECHANICAL ENGINEERING**  
**TKM COLLEGE OF ENGINEERING, KOLLAM**



**CERTIFICATE**

This is to certify that the project entitled “**CFD-ANALYSIS STUDY OF DRUG DEPOSITION IN TRACHEOBRONCHIAL AIRWAYS OF ASTHMATIC PERSONS FROM DIFFERENT AGE GROUPS**” submitted by **PRAFUL P, TKM21MECI11** to the APJ Abdul Kalam Technological University in partial fulfillment of the requirements for the award of the Degree of Master of Technology in Computer Integrated Manufacturing, Department of Mechanical Engineering is a bonafide record of the project work carried out by him under our guidance and supervision. This report in any form has not been submitted to any other University or institute for any purpose.

*Dr. K.E. Reby Roy*  
12/7/23

**Dr.K.E. Reby Roy**  
Internal Project Supervisor  
Professor  
Department of Mechanical Engineering  
TKM College of Engineering Kollam

*Prof. Kannan S.*  
12/7/23

**Prof. Kannan S.**  
Asst. Professor and PG Co-ordinator  
Department of Mechanical Engineering  
TKM College of Engineering Kollam

*Dr. Dileep P.N.*

**Dr.Dileep P.N.**  
Professor and Head  
Department of Mechanical Engineering  
TKM College of Engineering Kollam

## **ACKNOWLEDGEMENT**

First of all, I am indebted to GOD ALMIGHTY for giving me an opportunity to excel in my efforts to complete this project on time.

I am extremely grateful to **Dr. T.A. SHAHUL HAMEED**, Principal, TKM college of Engineering and **Dr. DILEEP P. N.** , Head of the Department, Department of Mechanical Engineering, for providing all required resources for successful completion of my project.

I am greatly obliged to my internal supervisor **Dr. K. E. REBY ROY**, professor, Department of Mechanical Engineering, for his encouragement, guidance and support.

My heartfelt gratitude to **Prof. KANNAN S.**, PG coordinator, Department of CIM **Prof. FAIZAL N. S.**, Assistant professor, Department of CIM for their valuable suggestions and guidance in the preparation of the project presentation and report.

I express my thanks to all Faculties and Technical staffs, Department of Mechanical Engineering, and all staff members and friends for all help and coordination extended in bringing out this project successfully in time.

I will be failing in duty if I do not acknowledge with grateful thanks to the authors of the references and other literatures referred to in this project.

Last but not the least, I am very much thankful to my parents who guided me in every steps which I took.

**PRAFUL P**

## **ABSTRACT**

The people who already had respiratory conditions like asthma were the ones who suffered the most from COVID. The most frequent chronic illness in children, asthma, is the main factor in pediatric hospitalizations all around the world. The inhalation of therapeutic drug particles is a widely used method for delivering drugs to treat lung covid after the person get infected. Understanding the transportation and deposition (TD) of inhaled drug particles in human lung airways is important for health risk assessment and therapeutic efficiency of targeted drug delivery for a covid affected person especially those who are already suffering from asthma. In this study, I have conducted cfd analysis of different lung geometry of healthy persons belonging to different age groups and compared it with the different lung geometry of persons who are affected by asthma. Here I took asthma condition in which there is a contraction of lung airway diameter of about 45%. I also conducted a cfd analysis to understand the penetration of corona, dpi and smi in the lung generation of G3-G6. The Experiment is conducted among the age group of 6years, 40years and 70 years. I drew a conclusion from the experiment conducted.

Keywords: Whole-lung-airway model (WLAM), Discrete Phase Model (DPM), Deposition Efficiency (DE), Dry Powder Inhaler (DPI)

# Contents

ABSTRACT

List of Tables

i

List of Figures

ii

ABBREVIATIONS

iii

1	INTRODUCTION	1
1.1	Outline of the process . . . . .	4
1.2	Objectives . . . . .	5
1.3	Scope . . . . .	5
1.4	Organisation of Report . . . . .	5
2	LITERATURE REVIEW	6
2.1	Overview . . . . .	6
2.2	SUMMARY . . . . .	15
3	LUNG AIRWAY GEOMETRY MODELLING	17
3.1	Overview . . . . .	17
3.2	Lung Model . . . . .	18
3.3	Numerical Method . . . . .	19
3.3.1	Airflow model. . . . .	20
3.3.2	Particle transport and deposition model. . . . .	23
3.3.3	Deposition efficiency calculation . . . . .	23
3.3.4	Grid dependency study and model validation. . . . .	25

4	RESULTS AND DISCUSSIONS	27
4.1	Overview	27
4.2	Comparison of different particle deposition	28
4.3	Drug deposition comparison in asthmatic persons of different age group	28
4.4	Airflow Velocity in Asthmatic person.	30
4.5	Wall-Shear distribution	31
4.6	Summary	31
5	CONCLUSION	33
5.1	Overview	33
5.2	Future Scope	34

## REFERENCES

## List of Tables

3.1	Lung Airway Dimension . . . . .	20
3.2	Physical properties of the particle and fluid phases . . . . .	25

## List of Figures

2.1 Drug Delivery Illustration[1] . . . . .	8
2.2 Tracheobronchial Generations[2] . . . . .	11
3.1 Airway model description[3] . . . . .	19
3.2 Lung Model created using CATIA V5. . . . .	21
3.3 Airflow representation in Ansys Fluent . . . . .	21
3.4 Airway Meshing in Ansys . . . . .	26
3.5 Airway Meshing of inlet in Ansys. . . . .	26
4.1 Deposition of particles in each generation. . . . .	28
4.2 Deposition of particles in Healthy vs Asthmatic . . . . .	29
4.3 Airflow velocity distribution. . . . .	30
4.4 Wall-Shear distribution . . . . .	31

## **ABBREVIATIONS**

WLAM	Whole-lung-airway model
DPM	Discrete Phase Model
DE	Deposition Efficiency
LES	Large Eddy Simulations
DPI	Dry Powder Inhaler
SMI	Soft Mist Inhaler

# Chapter 1

## INTRODUCTION

The SARS-CoV-2-induced global COVID-19 pandemic has impacted more than 223 nations, leading to a considerable number of fatalities, with the World Health Organization (WHO) reporting over 5,301,714 deaths as of December 14, 2021. Unfortunately, due to the emergence of new variants such as the Delta strain, which was initially discovered in India in October 2020, these figures are continuing to rise. SARS-CoV-2's primary target is the lungs, leading to oxygen deficiency and systemic inflammation, which can ultimately result in acute respiratory distress syndrome and damage to vital organs such as the kidneys, liver, heart, and brain.

The people who already had respiratory conditions like asthma were the ones who suffered the most from COVID. The most frequent chronic illness in children, asthma, is the main factor in pediatric hospitalizations all around the world. Since 1950, the prevalence of childhood asthma has significantly increased, especially in developing nations. This has had a negative impact on the children's quality of life and placed a significant financial burden on the family. It is important to understand the pathophysiology of pediatric asthma in order to successfully decrease and control the condition's explosive growth.[4]

Pulmonary infectious diseases have long been a significant threat to human life and global health. According to WHO data, pneumonia has been the leading cause of death among children, with an estimated 808,694 deaths of children under the age of five reported globally in 2017, accounting for 15% of child mortality. Tuberculosis (TB) remains one of the top 10 causes of death worldwide, with 1.6 million deaths attributed to TB in 2017, and over 10 million people currently living with the disease. The impact of pulmonary infectious diseases on a global scale is significant, imposing substantial social and economic burdens on society. However, there are significant challenges in finding effective and safe treatment options for these diseases.

In the case of SARS-CoV-2, apart from vaccines, certain drugs have entered the clinical stage and have demonstrated promising antiviral potential. REGEN-COV, a combination therapy consisting of two monoclonal antibodies (casirivimab and imdevimab), targets the receptor binding domain (RBD) on the spike protein of SARS-CoV-2 to prevent viral entry into host cells. It has been shown to reduce the duration of symptoms and decrease the risk of death without leading to virus mutations. Sotrovimab, an engineered human monoclonal antibody,

directly targets the spike protein of SARS-CoV-2, blocking its attachment and entry into human cells, thereby reducing the risk of disease progression in patients with mild to moderate COVID-19 infection. Remdesivir, the first officially approved small molecule drug for COVID-19 treatment in the United States, is a nucleoside analog prodrug that has proven effective in improving the recovery rate of moderate and severe COVID-19 patients in hospitals. However, its association with patient survival is less pronounced. Molnupiravir, an oral antiviral drug approved on an emergency basis by the FDA, increases the mutation rate in the viral genome, interrupting virus replication and spread. It can be used for the treatment of mild to moderate COVID-19 in adult patients. Another promising drug candidate is PF-07321332, an oral 3CL protease inhibitor that exhibits extensive antiviral activity against human coronaviruses in vitro. However, due to the rapid mutation of the virus, research and development of anti-SARS-CoV-2 drugs still have a long way to go. Some potential therapeutic compounds have failed in clinical trials due to issues like insufficient therapeutic concentrations at the target site and adverse effects resulting from off-target distributions.

For example, the potential use of chloroquine as a drug candidate for treating SARS-CoV-2 infection was initially considered due to its ability to inhibit viral replication and regulate immune response in vitro. However, its serious adverse effects, such as cardiotoxicity leading to ventricular arrhythmia, conduction block, and cardiovascular failure, have been associated with its use. The inappropriate use of chloroquine, especially among elderly patients or those with cardiovascular complications, can increase the risk of heart-related death. Moreover, the narrow therapeutic window of chloroquine makes it challenging to control its concentration within a safe range.

To address such therapeutic challenges, the development of drug delivery systems (DDS) to enhance site-specific drug accumulation or achieve precise delivery to the disease site becomes crucial.

Pulmonary drug delivery, among various delivery systems and strategies, offers distinct advantages, including no first-pass effect and high bioavailability, as it delivers therapeutics directly to lung lesions. With the ongoing pandemic, numerous antiviral pulmonary inhalations are currently undergoing clinical studies. This article review focuses on the physiological structure of the lungs, causes and changes associated with pulmonary infections, and explores pulmonary drug delivery strategies for the treatment of infectious lung diseases. Specifically, it discusses localized delivery systems for pulmonary administration, providing insights into the

future development of therapies for pulmonary infectious diseases and effective treatment alternatives.

The inhalation of aerosol particles is a widely used method for delivering drugs to treat lung diseases in humans. Therefore, it is imperative to study how particles are transported and deposited in the airways of the human lungs. This research is critical for ensuring the effectiveness of aerosol-based drug delivery and minimizing the health impacts of inhaled pollutants.

Extensive investigations have been conducted to analyze the airflow dynamics and particle deposition in non-realistic tracheobronchial lung airways. Researchers have developed lung models based on Weibel's model and symmetric triple bifurcation models to simulate airflow and particle deposition in specific generations. These studies have shown that microparticles tend to be deposited at cardinal angles due to their inertial impaction mechanism. On the other hand, nanoparticles exhibit more uniform deposition throughout the airways compared to microparticles.

Some researchers have utilized Large Eddy Simulations (LES) to study aerosol particle transport in lung models, revealing that a significant portion of particles is deposited in the upper airways through inertial impaction. However, these studies have mainly focused on the overall deposition efficiency without considering the deposition efficiency of individual generations.

The evolution of respiratory airway modeling has been thoroughly examined, providing valuable insights into the limitations of lung anatomy and the distribution of drugs in the lungs. Computational Fluid Dynamics (CFD) has proven to be an effective and accurate tool for predicting the local deposition efficiency of particles in the lung airways.

While previous studies have explored particle deposition in realistic lung models, the focus has primarily been on a limited number of generations. However, recent research has utilized computational fluid dynamics (CFD) simulations to investigate realistic lung models ranging from G0 to G6, revealing that microparticles tend to deposit in the upper tracheobronchial airways. Moreover, studies examining particle deposition in relation to temperature and humidity conditions have indicated that aerosol evolution occurs predominantly in the upper airway segments and over short timescales. Notably, the deposition efficiency of aerosol particles varies significantly with age, particularly during

childhood/teenage stages and in older individuals. Specifically, children tend to exhibit higher deposition efficiency in the mouth-throat section, whereas adults show the opposite trend in the pulmonary and alveolar sections. Nonetheless, limited research has been conducted on airflow dynamics and particle deposition in lung models for the elderly, despite the higher prevalence of lung diseases in this demographic. To enhance our knowledge of particle deposition in the lungs of older individuals, further investigations are necessary. Furthermore, conducting comprehensive studies of the entire lung has been challenging due to computational constraints and limitations. However, the present study employs a cutting method to facilitate CFD simulations of airflow and particle deposition in generations ranging from G0 to G14, while excluding generations beyond G14. This is due to the low airflow rate, which renders the inertial impaction deposition mechanism ineffective. By dividing the generations into five sections, each consisting of three generations, the continuity of airflow and particle numbers is maintained at the section boundaries. Overall, the primary objective of this study is to examine the impact of particle size and age on airflow and particle deposition at the micrometer scale in human lungs. The study assumes a consistent inhaled airflow rate for all ages, while accounting for variations in airway diameters based on age.

## 1.1 Outline of the process

The study of Cfd-Analysis Study of Drug Deposition in Tracheobronchial Airways of Asthmatic Person contain multiple steps. Here's a step-by-step outline of the process:

- Literature Review: Conduct a comprehensive review of existing literature and research related to lung airway models, drug delivery systems, different type drugs and their physical properties.
- Methodology: Selecting appropriate lung geometry, confirming the boundary conditions, finding the parameters.
- Validation: Validating the lung geometry with the previous works to confirm whether the designed model is working as per the standards.
- Analysis and Reporting: Producing different simulation results, analysing them, extracting the results and conclusion of the study conducted.

- Future Recommendations: Provide recommendations for further research and development such as introducing new geometry and boundary condition.

## 1.2 Objectives

The objectives of the CFD-Analysis Study of Drug Deposition In Tracheobronchial Airways of Asthmatic Persons From Different Age Groups are as follows:

- To investigate different particle size: The primary objective is to analyze and understand the deposition of different type of drug particle in the lung airway geometry.
- To investigate particle deposition of healthy persons in different age group: For the study, i am taking the age group of 6 years old, 40 years old and 70 years old. The particle deposition of a  $3\mu\text{m}$  drug particle has to be evaluated.
- To investigate particle deposition of asthma persons in different age group: For the study, i am taking asthma patients of the age group of 6 years old, 40 years old and 70 years old. The particle deposition of a  $3\mu\text{m}$  drug particle has to be evaluated.
- To compare and evaluate particle deposition in healthy and asthma persons: Comparitive study of healthy and asthma person to evaluate change in deposition efficiency.
- To evaluate the total experiment and reach a conclusion: Evaluating the comparison and deposition efficiency to suggest appropriate drug delivery system.

## 1.3 Scope

The scope of the work involves selecting lung geometry, conducting experimental tests, analyzing the simulations, proposing effective drug delivery strategies, comparing with existing strategy, and considering application-specific requirements.

## 1.4 Organisation of Report

The report is divided into five chapters, with the first chapter being the Introduction that covers the general background, objectives, and organization of the report. The second chapter reviews

the literature relevant to the project. The third chapter focuses on methodology, which is the main topic of study in the report. The chapter 5 is results. The final chapter is the conclusion.

## **Chapter 2**

### **LITERATURE REVIEW**

#### **2.1 Overview**

The objective of this paper is to provide a detailed and comprehensive literature review that focuses on pulmonary delivery strategies for the effective treatment of infectious lung diseases. Pulmonary drug delivery is an attractive option for targeted therapy due to its high bioavailability and the ability to bypass the first-pass effect. However, the complexity of the lungs, including their unique structural characteristics and biological barriers, requires careful consideration when designing drug delivery strategies. To understand the deposition of drug-loaded particles in the respiratory tract, *in vitro* and *in vivo* models have been developed and widely used in research.

Fungal pneumonia is infrequent, but its incidence is higher in people with weakened immune systems. Therefore, finding effective treatment options for this group of patients is crucial. In addition, metabolic enzymes present in lung epithelial cells can affect the breakdown and metabolism of therapeutic drugs, which may impact treatment outcomes. Therefore, it is essential to establish appropriate disease models to evaluate the efficacy of drugs against pulmonary infectious diseases. Researchers have developed both *in vitro* cell-based and *in vivo* animal models to conduct rigorous efficacy studies.

Moreover, the prevalence of drug-resistant strains of infectious agents continues to rise, highlighting the need for innovative treatment approaches. Pulmonary drug delivery has the potential to revolutionize the way we treat infectious lung diseases by precisely targeting the site of infection and achieving higher drug concentrations locally. This approach not only enhances therapeutic outcomes but also reduces systemic side effects, leading to improved patient compliance and overall treatment success.

However, the development of pulmonary drug delivery systems is not without challenges. The complexity of the lungs' anatomy and physiology demands careful consideration during formulation development and delivery design. Factors such as particle size, surface charge, and aerodynamic properties play critical roles in determining deposition patterns and drug absorption within the lungs. Clearance mechanisms in the respiratory tract can also affect drug retention and overall efficacy.

To overcome these challenges, researchers have employed various strategies, including particle engineering, the use of excipients, and novel drug carriers, to enhance drug delivery to the lungs. Inhalable formulations, such as dry powder inhalers and nebulizers, have gained popularity due to their ease of administration and ability to deliver a wide range of therapeutics. Additionally, advances in nanotechnology have opened up new possibilities for targeted drug delivery, allowing for precise drug localization and sustained release. In conclusion, it is important to note that the field of pulmonary drug delivery for infectious lung diseases is constantly evolving. This literature survey provides a comprehensive guide to the current research landscape in this field. The potential benefits of targeted lung delivery are significant, but it is imperative that researchers continue to address the associated challenges to ensure optimal therapeutic outcomes. By harnessing state-of-the-art technologies and engaging in interdisciplinary collaborations, the future of pulmonary drug delivery holds immense promise in revolutionizing the treatment of infectious lung diseases. Ultimately, this will lead to improved patient outcomes and global health.[1]

The introduction of the paper highlights the importance of simulating lung-aerosol dynamics to gain insight into toxic particle deposition and associated pulmonary disease treatment. It mentions that the majority of lung diseases are associated with occupational and environmental exposure to ambient aerosol pollutants, while inhalation of drug-aerosol is a modern way of targeting lung tumors and combating systemic diseases. However, due to the current computational resources available, it is impossible to simulate the transient 3-D aerosol dynamics in all 23 lung generations. Therefore, simplified configurations have to be considered which satisfy specific modeling requirements.[5] The paper presents a new whole-lung-airway model (WLAM) to simulate aerosol transport and deposition in the human respiratory tract. The model

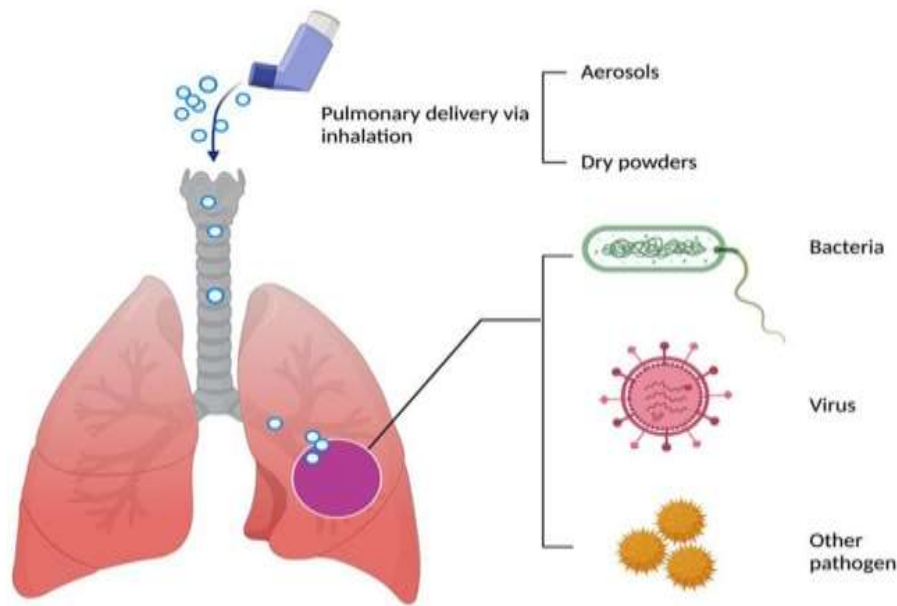


Figure 2.1: Drug Delivery Illustration[1]

represents the actual lung geometry via a basic 3-D mouth-to-trachea configuration while all subsequent airways are lumped together, i.e., reduced to an exponentially expanding 1-D conduit. The diameter for each generation of the 1-D extension can be obtained on a subject-specific basis from the calculated total volume which represents each generation of the individual. The alveolar volume was added based on the approximate number of alveoli per generation. A wall-displacement boundary condition was applied at the bottom surface of the first-generation WLAM, so that any breathing pattern due to the negative alveolar pressure can be reproduced. Specifically, different inhalation/exhalation scenarios (rest, exercise, etc.) were implemented by controlling the wall/mesh displacements to simulate realistic breathing cycles in the WLAM. The governing equations for airflow and particle transport were solved using a finite-volume method. The computational efficiency of the model was improved by using a hybrid EulerianLagrangian approach, which allowed for the simulation of a large number of particles with modest computational resources. The paper presents the results of the new whole-lung-airway model (WLAM) to simulate aerosol transport and deposition in the human respiratory tract. The model was validated by comparing the total and regional particle deposition results with experimental lung deposition results, and the outcomes provide critical insight to and quantitative results of aerosol deposition in human whole-lung airways with modest computational resources. The WLAM can be used in analyzing human exposure to toxic particulate matter or it can assist in estimating pharmacological effects of administered drug-

aerosols. The paper presents a new whole-lung-airway model (WLAM) to simulate aerosol transport and deposition in the human respiratory tract. The model was validated by comparing the total and regional particle deposition results with experimental lung deposition results, and the outcomes provide critical insight to and quantitative results of aerosol deposition in human whole-lung airways with modest computational resources. The WLAM can be used in analyzing human exposure to toxic particulate matter or it can assist in estimating pharmacological effects of administered drug-aerosols. The paper concludes that the new WLAM model is computationally efficient and can be used to predict particle deposition in the human respiratory tract with reasonable accuracy.

Rahman et al., discusses the effects of aging on airflow distribution and micron-particle transport and deposition in a human lung using a computational fluid dynamics (CFD) approach. The study investigates the particle transport and deposition in the lungs of people aged 50-70 years, using CFD. The paper mentions that the age-specific particle TD in human lungs, particularly in the aged, has not been well understood in literature. The introduction also highlights the importance of understanding particle transportation and deposition in human lung airways for health risk assessment and therapeutic efficiency of targeted drug delivery. The paper uses a computational fluid dynamics (CFD) approach to investigate the particle transport and deposition in the lungs of people aged 50-70 years. A new cutting method that splits the lung model into different sections has been developed as a feasible CFD method to simulate the particle TD in G0 to G14 lung airways. The inhalation of micron scale particles with three diameters ( $5\ \mu\text{m}$ ,  $10\ \mu\text{m}$  and  $20\ \mu\text{m}$ ) and a constant air flow rate in inhalation is considered. The airflow in lung airways is solved using software ANSYS FLUENT. The governing equations for airflow are the Reynolds-averaged Navier-Stokes (RANS) equations. The interaction of the continuous and discrete phases has been accomplished by the Discrete Phase Model (DPM) model. The study found that different sized particles are deposited in different generation airways. Nearly 100% of  $20\ \mu\text{m}$  particles are deposited in the upper lung airways (G0-G5) and no particles pass through G7. Particles can go into deeper airways as their diameter decreases. When the particle size is decreased to  $5\ \mu\text{m}$ , over 48% of particles can pass through G14 and enter the deeper lung airways. An increase in age causes more particles to deposit in the upper airway and fewer particles to enter the deeper airways. The paper concludes that the microparticles transport and deposition in the Tracheobronchial lung airway generations G0-G14 for 50-, 60-and 70-year-old lung models are investigated numerically. The airflow velocity in the airways increased with an increase in age due to the reduction of airway diameters. The

local increase in wall shear stress is observed in each bifurcation lung airway because the flow resistance happens in that area.

The study found that different sized particles are deposited in different generation airways.[6]

The introduction of the paper explains the importance of understanding the deposition of aerosol particles in the human lung airways for effective drug delivery and to measure the health implications of air pollution. The effectiveness of particle deposition as a drug delivery method depends on particle size, shape, and breathing capacity. Many researchers have studied nanoparticle deposition in human lung models to investigate the diffusion mechanism, and the results revealed that the percentage of nanoparticles deposited in the deep airways was greater than microparticles. The paper investigates the transportation and deposition of aerosol particles in the lungs of infants, children, and adults. The study found that less particles are deposited in upper lung airways than in lower airways in the lungs of all the three age groups. The results suggest that the particle deposition efficiency in lung airways increases with the decrease of particle size due to the Brownian diffusion mechanism. About 3% of 500 nm particles are deposited in airways G12-G15 for the three age groups. As the particle size is decreased to 5 nm, the deposition rate in G12-G15 is increased to over 95%. The present findings can help medical therapy by individually simulating the distribution of drug-aerosol for the patient-specific lung. The paper concludes that the deposition efficiency of particles in the human lung airways is significantly affected by lung airways reduction. The study found that the percentage of nanoparticles deposited in the deep airways was greater than microparticles. The present findings can help medical therapy by individually simulating the distribution of drug-aerosol for the patient-specific lung.[2]

Zhang et al., The paper is about the link between childhood asthma and air pollution. Childhood asthma is a common chronic disease that has rapidly increased since 1950, particularly in developing countries. Air pollution has been linked to childhood asthma, and children are more susceptible to the effects of air pollution on asthma morbidity due to their underdeveloped immune system and lung functions. Identifying the pathogenesis of asthma in children is important to reduce and control the rapid growth rate of childhood asthma. The present study employs a planar and symmetric model of airways for asthmatic children aged four years. The computational fluid dynamics (CFD) method was utilized to numerically investigate airflow and particle deposition in both the upper (G3-G6) and lower (G9-G12) conducting airways. Micron particles

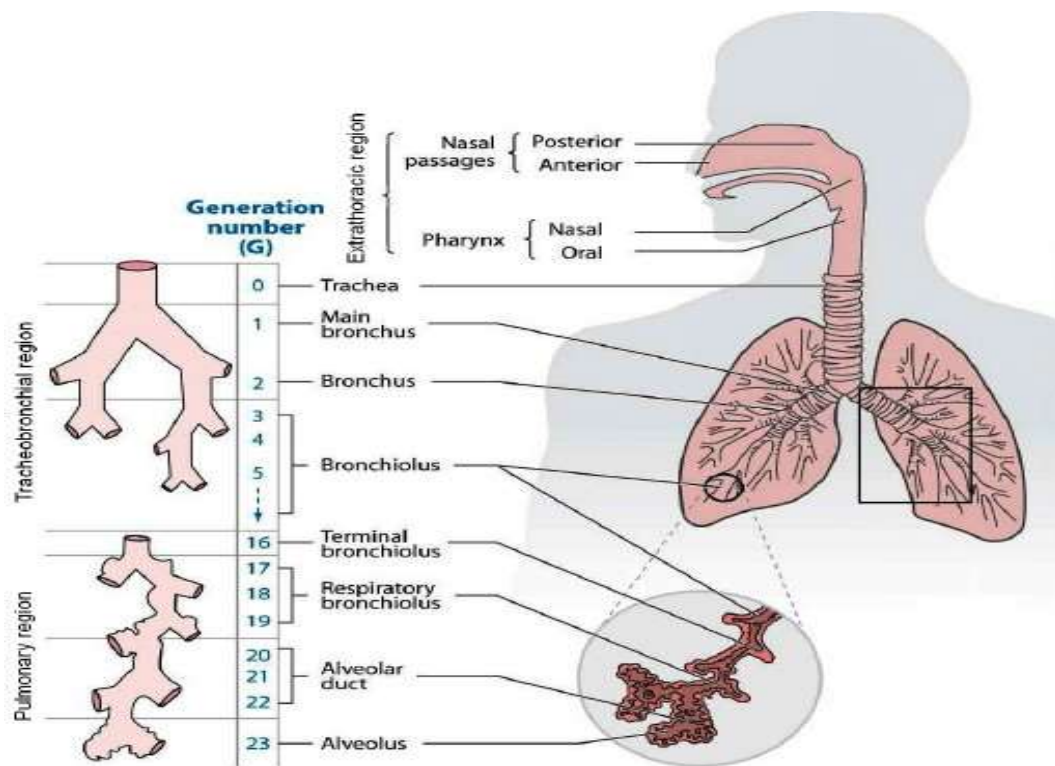


Figure 2.2: Tracheobronchial Generations[2]

ranging from  $1-10\mu\text{m}$  were examined. The deposition efficiency was quantified via deposition efficiency (DE), which was further divided into DE<sub>i</sub> (inertial impaction) and DE<sub>g</sub> (gravitational sedimentation) to examine the particle deposition due to different mechanisms. Furthermore, the study takes into account the severity of asthma by considering moderate (30% reduction in airway diameter) and severe (60% reduction) asthma. The present study has yielded the following findings: A marked increase in particle deposition was observed in asthmatic children in comparison to their healthy counterparts. Particle deposition efficiency exhibited a gradual increase with particle size among healthy children, while asthmatic children demonstrated a rapid increase. Larger particles were predominantly deposited in healthy children, whereas smaller particles were found to deposit in asthmatic children. In order to investigate particle deposition attributable to distinct mechanisms, the deposition efficiency was bifurcated into DE<sub>i</sub> (inertial impaction) and DE<sub>g</sub> (gravitational sedimentation). In healthy children, particles were deposited via inertial impaction and gravitational sedimentation in the upper and lower airways, respectively. Conversely, in asthmatic children, particles were deposited by inertial impaction solely. The severity of asthma was found to positively correlate with particle deposition in the airways. The narrowed airways led to increased particle deposition via inertial

impaction, which might serve as a biological pathogenesis responsible for the hospitalization of children with asthma.

The study highlighted the heightened susceptibility of asthmatic children to the adverse effects of particulate air pollution. It is recommended that avoiding exposure during air pollution events would constitute an effective measure to mitigate asthma attacks. The paper's conclusions suggest that there is a notable disparity between the deposition of particulate matters in the airways of asthmatic children and healthy children. This discrepancy is due to the increased airway narrowing that asthmatic children experience, which results in a greater particle deposition and subsequently leads to acute health effects and hospitalization. Furthermore, asthmatic children are more vulnerable to the impact of particulate air pollution, and therefore, it is advisable to avoid exposure during air pollution events as a practical and effective way to decrease the risk of asthma attacks in children.[7]

Weibel and Lorenz, 1966 discusses the physical events associated with the movement of gases in the lung and the use of refined models to reflect the properties of the airway system. The paper provides a literature survey of previous studies on airway models, including the use of simple airway models that did not need to be dimensionally defined, dimensional airway models proposed by Findeisen and Ross, and the need for new models of the human airway system based on the fundamental architectural pattern of dichotomy. The paper proposes two different models of the human airway system, one emphasizing the regular features of the airways and the other accounting for some of their irregularities. The paper provides numerical values of the airway dimensions of an average-sized adult human lung and lists equations and formulas for the over-all cross section and volume of the airways in each generation.[8]

The introduction of the paper explains that the deposition of aerosol particles in the airways depends on various factors such as the physical and hydrodynamic characteristics of the particles, inhalation flowrate, health state of the individual, and geometrical and morphological details of the airways. The paper discusses the efforts made in experiments and numerical simulations to determine deposition efficiencies and improve our understanding of airflow characteristics. The paper highlights the effects of flow turbulence in the conducting airways and how our understanding of it has improved over the years. The methods used in this paper involve Large Eddy Simulations (LES) to investigate the deposition of inhaled aerosol particles with diameters of 0.1, 0.5, 1, 2.5, 5, and 10  $\mu\text{m}$  in a reconstructed geometry of the human airways obtained via computed tomography. The paper assesses the effects of inlet flow

conditions, particle size, electrostatic charge, and flowrate. The paper introduces particle dimensionless numbers for the main deposition mechanisms, i.e. inertial impaction and electrostatic attraction, to indicate the relative importance between forces acting on a particle. The Stokes number ( $Stk$ ) is used to measure the relative importance of inertial effects in determining particle trajectories. The paper presents simulation results for the effects of the inlet velocity profile, inhalation flowrate, and electrostatic charge on particle deposition. The results show that using a more realistic inlet profile based on Laser Doppler Anemometry measurements resulted in enhanced deposition, mostly on the tongue. Increasing the inhalation flowrate from sedentary to activity conditions left the mean flowfield structures largely unaffected. Nevertheless, at the higher flowrates turbulent intensities persisted further downstream in the main bronchi. The overall Deposition Fractions (DF) increased with flowrate due to greater inertial impaction in the oropharynx for particle sizes greater than 2.5  $\mu$ m. Below 1.0  $\mu$ m, the DF was largely independent of particle size. Electrostatic charge increased the overall DF of smaller particles by as much as sevenfold, with most of the increase located in the mouth-throat. Moreover, significant enhancement in deposition was found in the left and right lung sub-regions of the reconstructed geometry. The paper concludes that there is a significant interplay between particle size, electrostatic charge, and flowrate, and in silico models should be customized for specific applications, ensuring all relevant physical effects are accounted for in a self-consistent fashion. The paper concludes that there is a significant interplay between particle size, electrostatic charge, and flowrate, and in silico models should be customized for specific applications, ensuring all relevant physical effects are accounted for in a self-consistent fashion. The paper also suggests that the use of increasingly sophisticated in silico models has improved our overall understanding of particle deposition in the human airways, but model realism remains elusive. The paper highlights the importance of understanding the multitude of factors that control pulmonary deposition in assessing the therapeutic or toxic effects of inhaled particles.

The introduction of the paper discusses the increasing popularity of respiratory drug delivery as an efficient way of administering medicine for both pulmonary and systemic pathogenic conditions. It highlights the advantages of this route of drug delivery over other noninvasive administration methods, especially for treating pulmonary lung diseases like asthma, COPD, cystic fibrosis, ARDS, and lung fibrosis. The introduction also mentions the rapid absorption of inhaled drug-aerosols through the large surface area of the alveolar lung

region into systemic circulation, resulting in rapid bio-distribution when targeting diseased organs.[9] The paper describes the use of a validated first-generation whole lung-airway model (WLAM) to analyze particle transport and deposition in a human respiratory tract model when a drug-aerosol is inhaled via a commercial dry powder inhaler (DPI). The DPI assumed for the study is the powder inhaler Novolizer, which has shown reproducible dosing capabilities. The validated modeling methodology was then employed to study the delivery of curcumin aerosols into lung airways using the Novolizer DPI for realistic mouth-inlet conditions. Once the base-case deposition results were established, the drug-air stream angle and the effective aerosol release area were changed to reduce excessive deposition in the oropharyngeal region. The study is the first to utilize CF-PD methodology to simulate drug-aerosol transport and deposition under actual breathing conditions in a whole lung model, using a commercial dry-powder inhaler for realistic inlet conditions. The paper reports the successful comparison of total as well as regional particle depositions in the WLAM, as inhaled from a DPI, with experimental data sets reported in the open literature. The validated modeling methodology was then employed to study the delivery of curcumin aerosols into lung airways using a commercial DPI. The study found that the use of a DPI leads to low lung deposition efficiencies because large amounts of drugs are deposited in the oral cavity. Hence, the output of a modified DPI has been evaluated to achieve improved drug delivery, especially needed when targeting the smaller lung airways. The study is the first to utilize CF-PD methodology to simulate drug-aerosol transport and deposition under actual breathing conditions in a whole lung model, using a commercial dry-powder inhaler for realistic inlet conditions. The paper concludes that the use of a dry powder inhaler (DPI) leads to low lung deposition efficiencies because large amounts of drugs are deposited in the oral cavity. Hence, the output of a modified DPI has been evaluated to achieve improved drug delivery, especially needed when targeting the smaller lung airways. The study is the first to utilize CF-PD methodology to simulate drug-aerosol transport and deposition under actual breathing conditions in a whole lung model, using a commercial dry-powder inhaler for realistic inlet conditions.

This paper presents experimentally determined total and regional deposition data for breathing monodisperse aerosols of a wide particle size range at different patterns through the mouth and nose. The authors derived simple analytical expressions for the efficiencies of the nasal passages, larynx, upper and lower ciliated thoracic airways, and the nonciliated portion of the lungs in collecting particles from inspired aerosols. Empirical expressions are now available for

the calculation of total and regional deposition in the human respiratory tract for particles of any size and density inspired at any pattern through the mouth or nose. The paper summarizes deposition data that have been accumulated in recent years at the laboratory. The principles of aerosol generation, characterization, and administration to the respiratory system and the principles of determining deposition have recently been summarized. Therefore, this paper will be confined to fundamental considerations of experimental studies of deposition in the healthy human respiratory tract with non-destructive, noninvasive techniques. In summary, this paper provides a comprehensive study of the deposition of particles in the human respiratory tract, including the derivation of analytical expressions for the efficiencies of different parts of the respiratory system in collecting particles from inspired aerosols.

## **2.2 SUMMARY**

The initial paper is a comprehensive review of literature regarding pulmonary drug delivery for the treatment of infectious lung diseases. It elucidates the benefits of pulmonary drug delivery, the challenges involved, and the techniques employed to augment drug delivery to the lungs. The second paper expounds upon a computational fluid dynamics (CFD) method utilized to study particle transport and deposition in the lungs of individuals aged 50-70 years. It investigates the deposition of particles of varying sizes in diverse airway generations and the repercussions of aging on particle deposition. The third paper posits two distinct models of the human airway system predicated on the fundamental architectural pattern of dichotomy. It furnishes numerical values of airway dimensions and equations for the overall cross-section and volume of airways in each generation. The fourth paper introduces a novel whole-lung-airway model (WLAM) for simulating aerosol transport and deposition within the human respiratory tract. It discusses the validation of the model and its potential applications in analyzing the human exposure to toxic particles and estimating the pharmacological effects of drug-aerosols. The fifth paper employs Large Eddy Simulations (LES) to scrutinize the deposition of inhaled aerosol particles within a reconstructed geometry of human airways. It inspects the effects of various factors, such as particle size, electrostatic charge, and flow rate, on particle deposition. The sixth paper deliberates on the escalating prevalence of respiratory drug delivery and the benefits of this route in treating pulmonary lung diseases. It describes the use of a verified whole-lung-airway model for analyzing particle transport and deposition when a drug-aerosol is inhaled via a commercial dry powder inhaler. The seventh paper presents data

regarding experimentally determined total and regional deposition for breathing aerosols of varying particle sizes and patterns through the mouth and nose. It provides analytical expressions for the efficiencies of diverse airway segments in collecting particles from inspired aerosols.

# **Chapter 3**

## **LUNG AIRWAY GEOMETRY**

### **MODELLING**

#### **3.1 Overview**

The initial lung geometries developed for simulating airflow in human lungs were primarily intended for adult use. However, as the deposition of drug particles varies significantly with age, particularly during childhood and adolescence, particle size decreases with increasing age. Xu and Yu conducted a theoretical calculation of aerosol particle deposition in the respiratory tracts of newborns, children, and adults, focusing on particles ranging from 0.01  $\mu\text{m}$  to 10  $\mu\text{m}$  in diameter. The study found that children have higher deposition efficiency in the mouth-throat section compared to adults, while the opposite was observed in the pulmonary and alveolar section. Patterson et al. investigated nanoparticle deposition in the respiratory tract of school-aged individuals (8 to 18 years old) and found that total particle deposition efficiency in the pulmonary section is higher for children than for older individuals. This higher deposition is attributed to the smaller lung size of school-aged individuals, which makes it easier for airborne particles to settle. Additionally, Deng et al. examined particle deposition in the tracheobronchial section of lung airways in infants, children, and adults (specifically 7-month-old infants, 4-year-old children, and 20-year-old adults) using computational fluid dynamics simulations. The study demonstrated that children have a higher deposition efficiency of microparticles compared to adults in the tracheobronchial section. While several studies have investigated airflow dynamics and particle deposition in lung models for younger populations, limited research has focused on older individuals. As people age, their lung volume and breathing capacity decrease. Kim et al. analyzed airflow dynamics in the lungs of elderly individuals and found that the pressure drop in the lung airways decreases by 38% between 80-year-olds and 50-year-olds. However, they did not investigate particle deposition in the elderly's lungs. Because lung diseases primarily affect older individuals and medications are often prescribed to this demographic, it is critical to enhance our understanding of particle deposition in their lungs. Furthermore, most studies investigating airflow and particle deposition in the lungs have only considered a limited number of generations (typically three or four). Due to the substantial computational time required, a comprehensive study of airflow dynamics and particle

deposition throughout the entire lung using computational fluid dynamics has never been conducted. In this study, we employed an efficient cutting method to enable CFD simulations of airflow and particle deposition from generations G0 to G14. The study excludes generations beyond G14 due to the low airway flow rate, which renders the inertial impaction deposition mechanism ineffective. The cutting method divides generations G0 to G14 into five sections, with each section encompassing three generations. The study aims to investigate the impact of particle size and age on airflow and particle deposition at the micrometer scale within the human lungs. The inhaled air flow rate remains the same for all ages, while the airway diameters vary with age.

### **3.2 Lung Model**

Three-dimensional (3D) lung models were created utilizing symmetric and planar lung airways spanning from generation G3 to G6 based on the proposed geometry by Xu and Yu [10]. Due to the unavailability of realistic lung models encompassing all generations from G3 to G6, simplified lung models were utilized as simulating such complex models would require computationally expensive resources. An efficient cutting method and simplified lung models were employed to gain insight into the fundamental mechanisms of particle deposition within a lung model containing multiple generations while keeping the computational time manageable. Although the solutions obtained in this study may differ quantitatively from realistic lungs, they will contribute to a better understanding of how particle deposition is influenced by particle size and age. Extensive research has been conducted on human lungs in individuals up to the age of 30, but obtaining straightforward lung geometries for older individuals presents a challenge. To address this, lung models for older individuals were generated based on the conclusions drawn

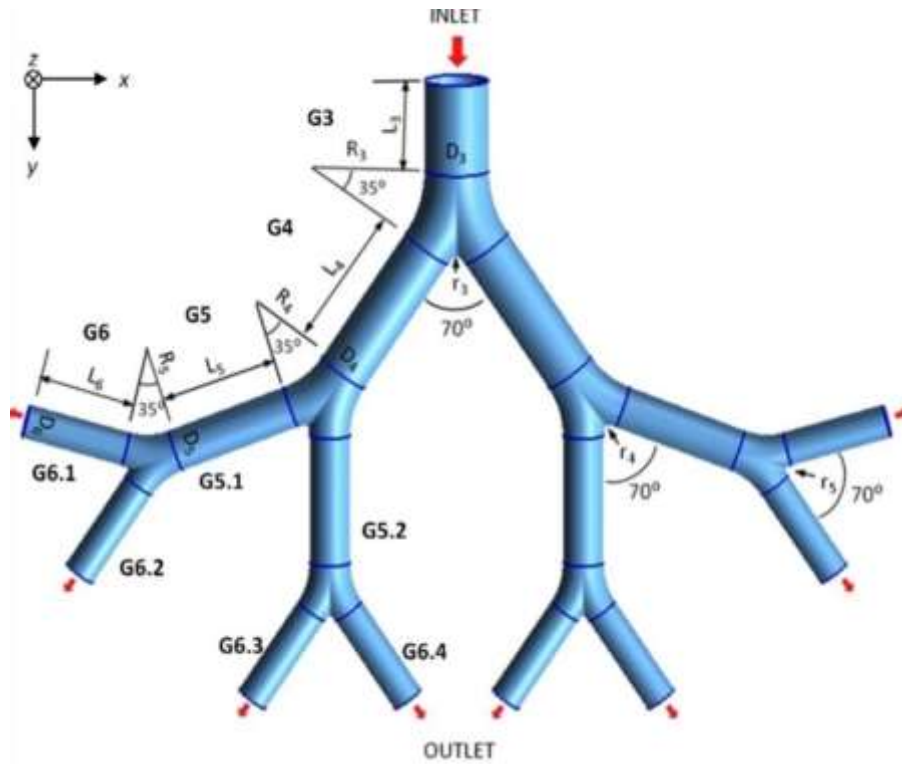


Figure 3.1: Airway model description[3]

from previous studies. The airway diameters of adult lungs show minimal changes between the ages of 30 and 50. Therefore, it was assumed that a 50-year-old lung has the same characteristics as a 30-year-old lung. 3D symmetric bifurcation lung airways for an individual in generations G3-G6 were created using Catia V5, as depicted in Figure 3.2, using the geometric parameters provided by Xu and Yu[10]. After 50 years of age in generations G3-G6, the airway diameter of each generation was reduced by 10% after every 10-year age increment. Additionally, the size of the alveolar sacs increases with age due to changes in tissue parameters and lung morphology resulting from aging. Lung tissue becomes approximately 7% stiffer between the ages of 50 and 80, leading to increased lung compliance. Lung compliance is a volumetric value dependent on lung size and refers to the lung's elastic property. Generally, as people age, their lungs become more compliant. Examining lung compliance aids in understanding the elastic characteristics associated with aging. The geometric parameters of the lung airways are detailed in the provided table. Generation G0 features one bifurcation, and the number of bifurcations for the  $n$ th generation is  $2n$ . Simulating the airflow in all generations from G0 to G14 without simplification using computational fluid dynamics (CFD) would be computationally infeasible. To ensure affordable computation time, I focused on G3-G6 and their corresponding

Table 3.1: Lung Airway Diameter

Generation	Diameter(mm)		Length(mm)
	40 years old	45% constricted	
3	5.6	3.08	7.59
4	4.5	2.475	12.68
5	3.5	1.925	10.71
6	2.8	1.54	9.01

Generation	Diameter(mm)		Length(mm)
	70 years old	45% constricted	
3	4.48	2.464	7.59
4	3.6	1.98	12.68
5	2.8	1.54	10.71
6	2.24	1.232	9.01

Generation	Diameter(mm)		Length(mm)
	6 years old	45% constricted	
3	3.5	1.925	4.4
4	2.9	1.595	7.3
5	2.3	1.265	6.2
6	1.9	1.045	5.2

geometries, as illustrated in the figure. Airflow and particle simulation were conducted separately for each section while maintaining continuity of air mass and particle mass at the interfaces between generations.

### 3.3 Numerical Method

#### 3.3.1 Airflow model

The airflow in lung airways is solved using software ANSYS FLUENT. The governing equations for airflow are the Reynolds averaged Navier-Stokes (RANS) equations:

$$\frac{\partial \rho}{\partial t} + \frac{\partial}{\partial x_i} (\rho \bar{u}_i) = 0 \quad (3.1)$$

$$\frac{\partial}{\partial t} (\rho \bar{u}_i) + \frac{\partial}{\partial x_j} (\rho \bar{u}_i \bar{u}_j) = - \frac{\partial p}{\partial x_i} + \frac{\partial}{\partial x_j} \left[ \mu \left( \frac{\partial \bar{u}_i}{\partial x_j} + \frac{\partial \bar{u}_j}{\partial x_i} \right) \right] + \frac{\partial}{\partial x_j} (-\rho \overline{u'_i u'_j}) \quad (3.2)$$

the fluid velocity is denoted by  $\vec{u}$ , while molecular viscosity is represented by  $\mu$ . The fluid density is  $\rho$ , and air pressure is  $p$ . The Reynolds stresses related to turbulence model are expressed as

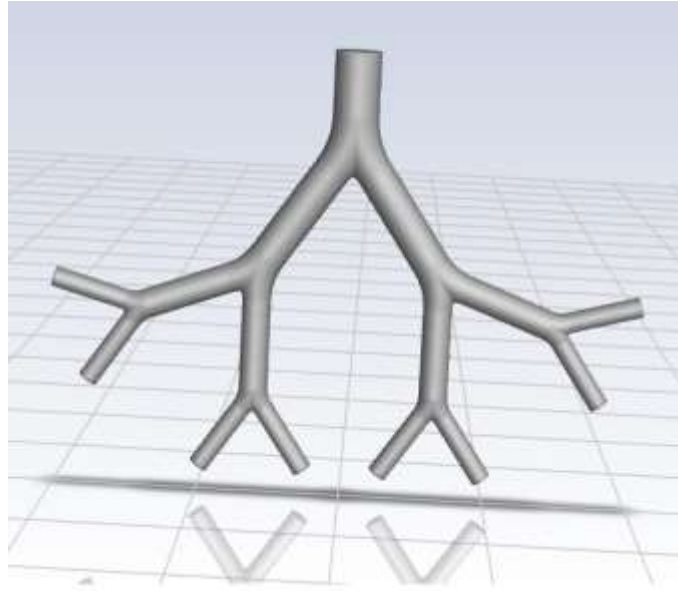


Figure 3.2: Lung Model created using CATIA V5

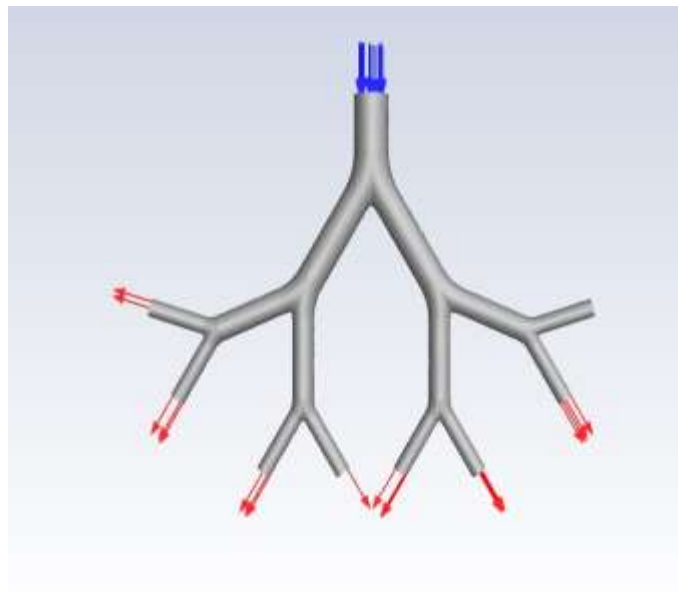


Figure 3.3: Airflow representation in Ansys Fluent

$\overline{\rho u'_i u'_j}$ . To simulate turbulence, the realisable k- $\epsilon$  turbulence model is utilized, which has been demonstrated to perform better than the standard k- $\epsilon$  model under various flow conditions, such as rotating homogeneous shear flows, boundary-free shear flows, channel and flat boundary layer flows with or without pressure gradients, and backward facing step flows. Furthermore, the realisable k- $\epsilon$  model has been shown to accurately predict the mean flow rate of complex lung geometries.

The RANS equations were solved using a combination of the second-order upwind and pressure-velocity coupling schemes. The triple bifurcation symmetric lung airway model was utilized, with the velocity inlet and pressure outlet boundary conditions being given. The inlet boundary velocity was predetermined, while a zero gauged pressure condition was applied at the exits. Existing studies have explored the effects of unsteady inhalation profiles on particle TD in unsteady flows. However, in this particular instance, a constant velocity was employed at the inlet boundary of each section to test the efficacy of the current cutting method, without the influence of velocity variations. The airway wall was assumed stationary, and the wall surfaces of the airways were treated as no-slip walls. The RANS equations were solved using a combination of the second-order upwind and pressure-velocity coupling schemes. The triple bifurcation symmetric lung airway model was utilized, with the velocity inlet and pressure outlet boundary conditions being given. In each section of Fig.3.2, the inlet boundary velocity was predetermined, while a zero gauged pressure condition was applied at the exits. Existing studies have explored the effects of unsteady inhalation profiles on particle TD in unsteady flows. However, in this particular instance, a constant velocity was employed at the inlet boundary of each section to test the efficacy of the current cutting method, without the influence of velocity variations. The airway wall was assumed stationary, and the wall surfaces of the airways were treated as no-slip walls.

If the assumption is made that the flow rate of inhaled air is uniformly distributed amongst all  $2^n$  bifurcations pertaining to generation G-n, then it can be deduced that the inlet flow rate of each bifurcation belonging to G-n is  $Q_n^i = Q/2^n$ , where Q represents the inlet flow rate at G0. As a result, the inlet velocity of each section originating from G-n can be computed through the following formula:

$$u = Q_n^i / A_n \quad (3.3)$$

where  $A_n$  is the cross-sectional area of the inlet

### 3.3.2 Particle transport and deposition model

The current model under consideration is a one-way coupling model that solely accounts for the transportation of particles in the air flow, excluding the influence of the particles on the airflow. When the volume concentration of the particles surpasses 15%, two-way models that take into account particle-particle interaction become necessary. Nonetheless, in all drug delivery applications, the volume concentration remains significantly below 15%. In order to replicate the transportation of suspended, dilute particles in the human lung, collision-free conditions can be implemented, or alternatively, particle-particle interaction can be disregarded. A majority of the published literature has not taken into account particle-particle interaction, as direct interaction can be overlooked under conditions where the particle suspension entering the tracheobronchial airway is dilute. This study has accomplished the interaction between the continuous and discrete phases through employment of the Discrete Phase Model (DPM) model.

The Lagrangian methodology is employed for the purpose of ascertaining the particle TD within the airways of the human lung. The equation of force balance pertaining to every single particle is depicted as such:

$$\frac{d\vec{u}_p}{dt} = F_D (\vec{u} - \vec{u}_p) + \frac{\vec{g}}{\rho_p} (\rho_p - \rho) \quad (3.4)$$

where the fluid and particle velocities are denoted by  $\vec{u}$  and  $\vec{u}_p$ , respectively, the gravitational acceleration is represented by  $\vec{g}$ , and  $\rho_p$  refers to the particle density, which is determined to be  $1100 \text{ kg/m}^3$ . The drag force per unit particle mass is given by  $F_D(\vec{u} - \vec{u}_p)$ , while the coefficient  $F_D$  is computed using a the formula:

$$F_D = \frac{18\mu}{\rho_p d_p^2} C_D \frac{Re_p}{24} \quad (3.5)$$

where  $C_D$  is the drag coefficient

### 3.3.3 Deposition efficiency calculation

The n-th generation's regional deposition efficiency is defined as the proportion of particles captured (trapped) in the airways of this generation, out of the particles dispersed at the inlet boundary of each section. It is symbolized by  $\eta_{L,n}$ , where the subscript n denotes the generation number. For the simulations, 79,800 uniformly sized spherical particles were randomly

introduced from the inlet surface at one time per section inlet. The deposited particle figures are then transformed using Eq.(3.6) based on the local deposition efficiency.

$$\eta_{L,n} = \frac{\text{Number of particles are trapped in a lung airways}}{\text{Total number of particles released at the inlet of this section}} \quad (3.6)$$

In the pulmonary system, the first fourteen generations of airways, denoted as G0-G14, are distinctly compartmentalized into five sections. The concentration of particles at the inlet boundary of each section experiences a decremental trend as compared to the previous section, primarily due to the absorption of particles in the preceding section. Consequently, the determination of the global deposition efficiency ( $\eta_n$ ) of the n-th section necessitates the application of the following formula:

$$\eta_n = \eta_{L,n} \times (1 - \sum_{i=1}^K \eta_i) \quad (3.7)$$

where K stands for the number of generations in all the previous sections. The percentage of particles that escape from all the outlets of each generation and enter the deeper lung is defined as particle escaping rate. The formula for calculating the particle escaping rate of generation n( $\alpha_n$ ) is:

$$\alpha_n = 1 - \sum_{i=1}^n \eta_i \quad (3.8)$$

The inlet at G3 is defined as velocity inlet and outlets at G7 is defined as pressure outlet. Standard k-omega turbulent model is used with inlet flow rate of 30L/min and zero pressure outlets. Escape type Discrete Phase BC is implemented at inlet and outlet face, and at wall trap BC type is implemented. The walls are assumed to stationary and no slip. SIMPLE algorithm was used to solve the coupling between velocity and pressure. Terms of governing equations were discretized with second order upwind scheme and also pressure value interpolation was second order. As reported by (Velavan and Meyer, 2020)[11], coronaviruses such as COVID-19, have a mean size of between 65 and 125 nm, with an envelope diameter of 80 nm and spikes measuring is at about 20 nm. The dimensions of aerosols coming out during coughing and sneezing are vital in ascertaining airborne disease transmission. In healthy and diseased individuals their sizes may vary.SARS-CoV-2 is currently thought to spread mostly by respiratory droplets. Large respiratory particles with a diameter of more than 5 to 10 m are typically referred to as respiratory droplets. When persons are in close proximity (within one meter), or due to fomite transmission in the nearby environment, SARS-CoV-2 can be spread through droplets. Physical properties of all particles used in the simulation is given in Table 3.2.[12]

Table 3.2: Physical properties of the particle and fluid phases

Phase		Property	Value
Fluid (air)		Viscosity Density	1.7894e-5 kg (m s) <sup>-1</sup> 1.225 kg/m <sup>3</sup>
Particle	Corona ( <u>water-liquid</u> )	Diameter Density	5 μm 998.2kg/m <sup>3</sup>
	DPI (anthracite)	Diameter Density	3 μm 1550 kg/m <sup>3</sup>
	SMI ( <u>water-liquid</u> )	Diameter Density	3 μm 998.2 kg/m <sup>3</sup>

### 3.3.4 Grid dependency study and model validation

The assessment of grid dependency is executed through the performance of numerical simulations on G3-G6 at  $dp = 10\mu\text{m}$ , utilizing six meshes that possess identical structures but vary in mesh densities. The minimum grid sizes adjacent to the wall for Mesh 1 and Mesh 6 are 0.8 mm and 0.235 mm, respectively. The node numbers for Meshes 1-6 range from 172,726 to 865,461. Figure illustrates the mesh in proximity to a bifurcation of generation G4. To ensure accurate prediction of the wall boundary flow within the lung airway, ten-layers of smooth inflation are implemented near the wall, as depicted in Figure. The mesh structure for all other generations is akin to that which is shown in Fig. 3.4.

The current Computational Fluid Dynamics (CFD) technique has been verified by means of available published records of airflow and particle Total Deposition (TD) in G3-G6 at  $Re = 1000$  and  $2000$ . The inhalation flow rates of 3.87 liters per minute ( $Re = 1000$ ) and 7.78 liters per minute ( $Re = 2000$ ) have been computed, taking into account the inlet diameter of G3. The simulations have been executed for particle sizes ranging from  $1\mu\text{m}$  to  $10\mu\text{m}$  in diameter, including  $dp=1\mu\text{m}$ ,  $3\mu\text{m}$ ,  $5\mu\text{m}$ ,  $6\mu\text{m}$ ,  $7\mu\text{m}$ ,  $8\mu\text{m}$ , and  $10\mu\text{m}$ .

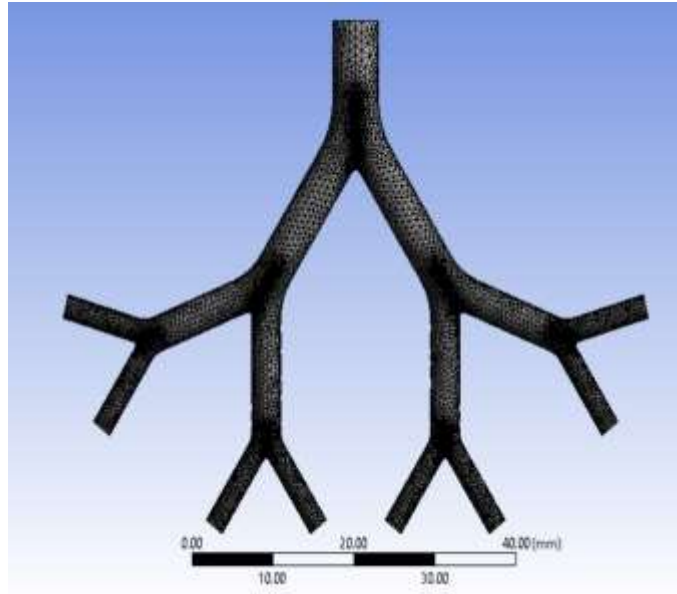


Figure 3.4: Airway Meshing in Ansys

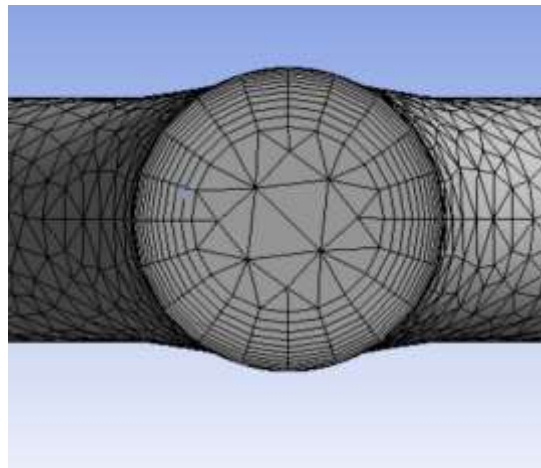


Figure 3.5: Airway Meshing of inlet in Ansys

## Chapter 4

# RESULTS AND DISCUSSIONS

### 4.1 Overview

In this particular study, the inhalation flow airflow rate of  $Q = 45\text{L}/\text{min}$  at G0 is being considered for individuals between the ages of 40 and 70, while for 6-year-olds,  $Q = 8\text{L}/\text{min}$ . It must be noted, however, that the inhalation velocity profile plays a crucial role in the calculation of particle deposition in human lung airways. Kadota et al.[13] conducted a study on the constant and inhalation flow pattern to calculate particles deposition in a realistic human airway. Similarly, Ahookhosh et al. [14], investigated an experimental approach for particles deposition in a realistic lung model of generations mouth to four (G4), while considering three constant flow rates. The results of this study have shown that the deposition density increased with an increased flow rate. Additionally, it is important to bear in mind that the inhalation route (mouth and nasal) has a significant impact on the particle deposition in the upper and tracheobronchial lung airways.[15] Nevertheless, the results have indicated that the inhaling route did not have any effect on the distribution of deposited particles downstream of the trachea.

Hence, alterations in lung geometry for varying ages of individuals result in modifications to inlet velocity. Age-related decline in lung function has been documented and is contingent on breathing parameters, including tidal volume and breathing frequency. Specifically, breathing frequency for 6-year olds, 40-year olds, and 70-year olds is 16 per minute, 13.65 per minute, and 12.92 per minute, respectively. Additionally, tidal volumes for 6-year olds, 40-year olds, and 70-year olds are 150 ml, 500 ml, and 179 ml, respectively.[16]

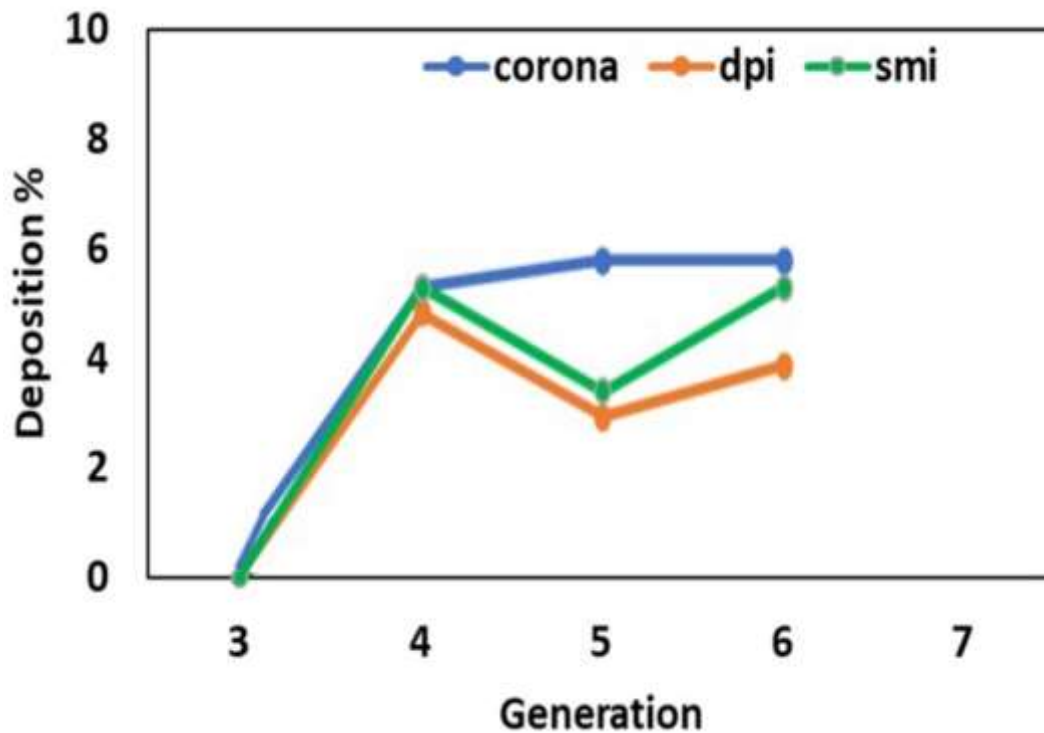


Figure 4.1: Deposition of particles in each generation

## 4.2 Comparison of different particle deposition

We can clearly see where the particles reach and the different deposition patterns of particles in varying diameters. The graph in fig 4.1 shows the deposition percentages of each generation. There is no particle deposit at G3, and small amount of particles deposit at the first bifurcation (G4), but a greater number of particles deposit at G5 and in G6, in all models. For each generation from G3 to G6 the percentage of deposition is increasing that may be because of reduction in airway diameter and gravitational effect. The study focuses on the airflow inhalation of a total of 4 generations with one inlet and 8 outlets. Particles that are not deposited are escaped through the outlet and may deposit in the successive generations of airways.

## 4.3 Drug deposition comparison in asthmatic persons of different age group

Fig 4.2 shows the particle deposition in the upper (G3-G6) conducting airways among healthy persons and asthmatic persons with 45% constricted conditions. We found that particle de-

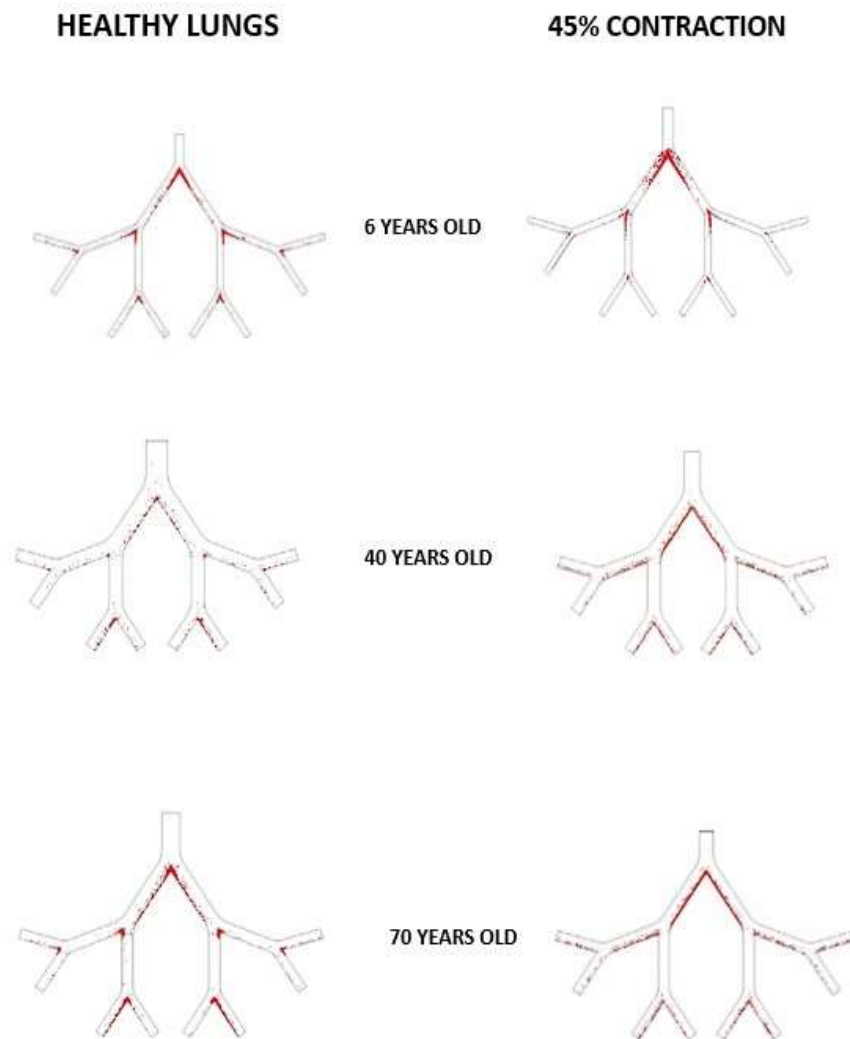


Figure 4.2: Deposition of particles in Healthy vs Asthmatic

position was significantly increased in asthmatic persons as compared with healthy persons. Particle deposition efficiency increased rapidly for asthmatic persons. We found that a mainly large number of particles were deposited in 45% constriction, which indicates that particles become easier to deposit in the upper airways as the constriction degree increases. The inhalation flow airflow rate of  $Q = 45\text{L}/\text{min}$  at  $G_0$  is being considered for individuals between the ages of 40 and 70, while for 6-year-olds,  $Q = 8\text{L}/\text{min}$ . We can see that there is an increase of more than 50% in deposition in the asthmatic lungs.

## 4.4 Airflow Velocity in Asthmatic person

The path lines for the symmetric Weibel model for G3-G6 are shown in Fig 4.3. Initially, the incoming airflow splits at the first bifurcation and the boundary layer appears at the inside wall of the first daughter tube (G4). An axial airflow rate is found more in one of the branches of

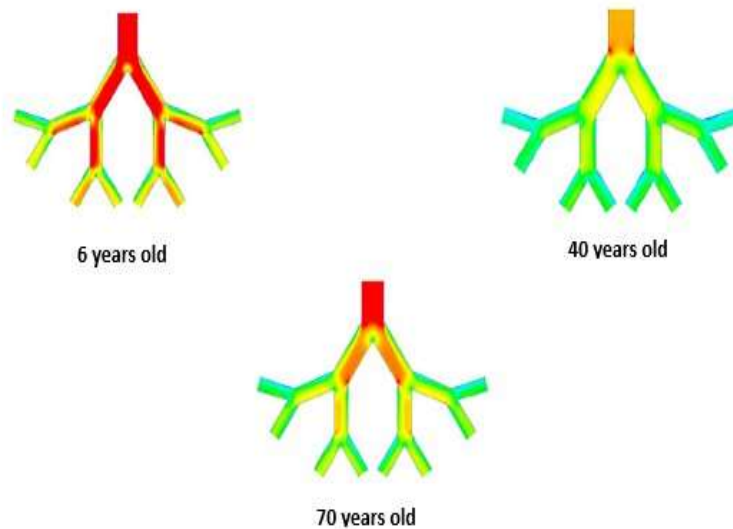


Figure 4.3: Airflow velocity distribution

G5 and transfers to the next daughter branch. The particle gets deposited at the wall where the velocity is smaller than the center lines. The velocity distribution and maximum velocities have increased may be due to the 45% constriction in the diameter of the airway. The air is entered through the upper side of G3 and goes out through 8 outlets at the bottom of G6. Since it is symmetric, the same values are obtained at the same generations that are branched into opposite sides. The velocity is reducing gradually from G3 to G6 and minimum velocity showed near the wall.

## 4.5 Wall-Shear distribution

Wall shear stress is the tangential force exerted by the fluid on the wall surface. The maximum values are obtained at the inlet of airways. For fig 4.4 (a), (b) and (c) the shear stress is equally distributed, and it depends on the air viscosity and velocity distribution. Since the air viscosity is low, the wall shear stress has also become low. Wall shear stresses in human airways release

the Adenosine triphosphate (ATP) and also intracellular calcium and are responsible for inducing the disease defense mechanism. Low-level shear stress led to an inverse relationship with the permeability of epithelial cells, while excessive wall shear stress can cause epithelial damage. It shows that the wall shear at the top of the inlet surface is the maximum and visible shear

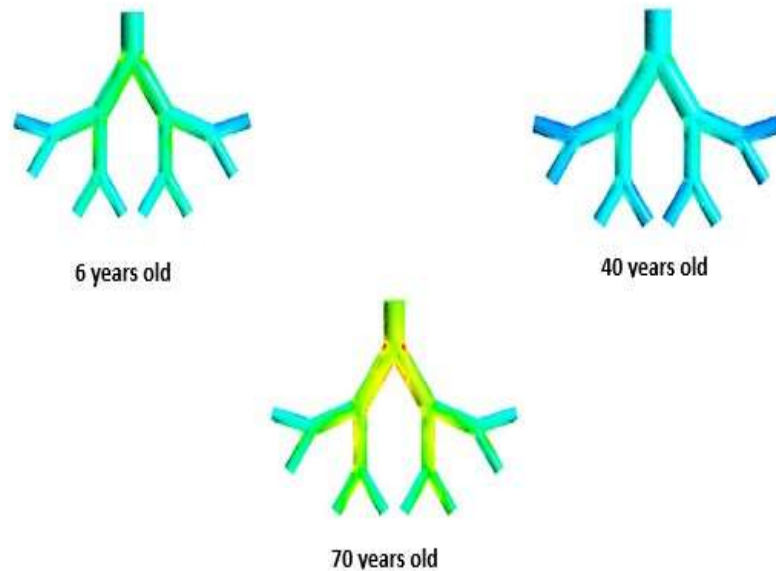


Figure 4.4: Wall-Shear distribution

stress found at each bifurcation also. The overall wall shear for the k- turbulent model is almost similar.

## 4.6 Summary

In this study the CFD analysis is conducted to determine how aging affects the deposition of pharmaceutical drug particles in the tracheobronchial airways of human lung. At first we checked the deposition percentage of each type of particles in each generation shows the corona particles are distributed to all the generations which indicates the particles may be able to distribute effectively to all the regions in the lung since. Particle size is also significant in distribution, if the particles are of lower size it will distribute mainly to the upper lobes of lung

while the corona particles are relatively of larger size so it can be distributed to the lower lobar regions due to the inertial effects.

The main part of study was to analyse the distribution of drug particle in healthy lung of different age group versus the deposition in asthmatic lung. The inhalation flow airflow rate of  $Q = 45\text{L/min}$  at G0 is being considered for individuals between the ages of 40 and 70, while for 6-year-olds,  $Q = 8\text{L/min}$ . We can see that there is about a increase of more than 50% in deposition in the asthmatic lungs.

## Chapter 5

# CONCLUSION

### 5.1 Overview

This Study presents the results of particle deposition and airflow of pharmaceutical drugs and corona particles in adult human respiratory airways G3-G6. It was found that airflow in all models is similar, and the pressure drop from 10 Pa to 0 Pa influence the particles to move with the inhaled air velocity. In this study, only structural and physical characteristics are discussed. The chemical behavior of each pharmaceutical drug may be different. Around 7% of corona particles are deposited on the walls of airways of G3-G6 and the rest of the particles are escaped through the outlet and go to daughter airways for further deposition. By looking at the trend of deposition pattern in G3-G6, the deposition may increase in the daughter airways of up to 2-4%. Since the size of the particle is lower than the size of the above-mentioned aerosol, more percentage of DPI particles and SMI particles are deposited on the daughter airways wall and the rest of the particles are escaped and may go up to the alveolar region. Both DPI and SMI have good deposition in the airways and can be used as a drug-delivery device for fighting corona. The maximum velocity of 3.5 m/s is obtained for particle size of  $3\mu\text{m}$  than that of  $5\mu\text{m}$ .

The study of analysis of the distribution of drug particle in the healthy lung of different age group versus the deposition in asthmatic lung show that there is a significant increase in deposition efficiency due to the constriction of size by 45%, we can see that the deposition has increased by about 50%. The inhalation flow airflow rate of  $Q = 45\text{L}/\text{min}$  at G0 is being considered for individuals between the ages of 40 and 70, while for 6-year-olds,  $Q = 8\text{L}/\text{min}$  remained same for the asthmatic lung model, therefore there is a slight increase in velocity and pressure.

The drug particle inside DPI and SMI may kill the virus or may prevent virus infection that depends on the drug's chemical composition and properties. But as in the literature DPI needs high inhalation power so patients with existing lung diseases or aged people may find it difficult to use. And as there is increase in deposition efficiency in the upper generation, it will better to use drug which has higher chance of penetration to the inner lungs.

## **5.2 Future Scope**

Future research should address some of this study's weaknesses. The modeling of particle TD first simply took the inhaling condition into account. In the upcoming research, I will take both the inhaling and exhalation processes into account for particle deposition by introducing a moving mesh. In addition, I took into account varied micron-size particle deposition in the G3-G6 in future research.

## REFERENCES

- [1] S. He, J. Gui, K. Xiong, M. Chen, H. Gao, and Y. Fu, “A roadmap to pulmonary delivery strategies for the treatment of infectious lung diseases,” *Journal of nanobiotechnology*, vol. 20, no. 1, p. 101, 2022.
- [2] M. M. Rahman, M. Zhao, M. S. Islam, K. Dong, and S. C. Saha, “Aerosol particle transport and deposition in upper and lower airways of infant, child and adult human lungs,” *Atmosphere*, vol. 12, no. 11, p. 1402, 2021.
- [3] C. Ou, J. Hang, Q. Deng *et al.*, “Particle deposition in human lung airways: effects of airflow, particle size, and mechanisms,” *Aerosol and Air Quality Research*, vol. 20, no. 12, pp. 2846–2858, 2020.
- [4] S. Choi, S. Miyawaki, and C.-L. Lin, “A feasible computational fluid dynamics study for relationships of structural and functional alterations with particle depositions in severe asthmatic lungs,” *Computational and mathematical methods in medicine*, vol. 2018, 2018.
- [5] J. Wang, Y. Zhang, X. Chen, Y. Feng, X. Ren, M. Yang, and T. Ding, “Targeted delivery of inhalable drug particles in a patient-specific tracheobronchial tree with moderate covid-19: A numerical study,” *Powder Technology*, vol. 405, p. 117520, 2022.
- [6] M. M. Rahman, M. Zhao, M. S. Islam, K. Dong, and S. C. Saha, “Aging effects on airflow distribution and micron-particle transport and deposition in a human lung using cfd-dpm approach,” *Advanced Powder Technology*, vol. 32, no. 10, pp. 3506–3516, 2021.
- [7] W. Zhang, Y. Xiang, C. Lu, C. Ou, and Q. Deng, “Numerical modeling of particle deposition in the conducting airways of asthmatic children,” *Medical Engineering & Physics*, vol. 76, pp. 40–46, 2020.
- [8] E. R. Weibel and E. R. Weibel, “Geometric and dimensional airway models of conductive, transitory and respiratory zones of the human lung,” *Morphometry of the human lung*, pp. 136–142, 1963.

- [9] R. Dalby, M. Spallek, and T. Voshaar, "A review of the development of respimat® soft mist™ inhaler," *International journal of pharmaceuticals*, vol. 283, no. 1-2, pp. 1–9, 2004.
- [10] G. Xu and C. Yu, "Effects of age on deposition of inhaled aerosols in the human lung," *Aerosol science and Technology*, vol. 5, no. 3, pp. 349–357, 1986.
- [11] L. A. Nikolai, C. G. Meyer, P. G. Kremsner, and T. P. Velavan, "Asymptomatic sars coronavirus 2 infection: Invisible yet invincible," *International Journal of Infectious Diseases*, vol. 100, pp. 112–116, 2020.
- [12] B. U. Lee, "Minimum sizes of respiratory particles carrying sars-cov-2 and the possibility of aerosol generation," *International journal of environmental research and public health*, vol. 17, no. 19, p. 6960, 2020.
- [13] K. Kadota, N. Inoue, Y. Matsunaga, T. Takemiya, K. Kubo, H. Imano, H. Uchiyama, and Y. Tozuka, "Numerical simulations of particle behaviour in a realistic human airway model with varying inhalation patterns," *Journal of Pharmacy and Pharmacology*, vol. 72, no. 1, pp. 17–28, 2020.
- [14] K. Ahookhosh, S. Yaqoubi, M. Mohammadpourfard, H. Hamishehkar, and H. Aminfar, "Experimental investigation of aerosol deposition through a realistic respiratory airway replica: an evaluation for mdi and dpi performance," *International journal of pharmaceuticals*, vol. 566, pp. 157–172, 2019.
- [15] F. Lizal, J. Elcner, J. Jedelsky, M. Maly, M. Jicha, Á. Farkas, M. Belka, Z. Rehak, J. Adam, A. Brinek *et al.*, "The effect of oral and nasal breathing on the deposition of inhaled particles in upper and tracheobronchial airways," *Journal of Aerosol Science*, vol. 150, p. 105649, 2020.
- [16] W. Hofmann, "Mathematical model for the postnatal growth of the human lung," *Respiration physiology*, vol. 49, no. 1, pp. 115–129, 1982.